

RSC Advances



This is an *Accepted Manuscript*, which has been through the Royal Society of Chemistry peer review process and has been accepted for publication.

Accepted Manuscripts are published online shortly after acceptance, before technical editing, formatting and proof reading. Using this free service, authors can make their results available to the community, in citable form, before we publish the edited article. This *Accepted Manuscript* will be replaced by the edited, formatted and paginated article as soon as this is available.

You can find more information about *Accepted Manuscripts* in the [Information for Authors](#).

Please note that technical editing may introduce minor changes to the text and/or graphics, which may alter content. The journal's standard [Terms & Conditions](#) and the [Ethical guidelines](#) still apply. In no event shall the Royal Society of Chemistry be held responsible for any errors or omissions in this *Accepted Manuscript* or any consequences arising from the use of any information it contains.



Journal Name

ARTICLE

Lithium doped Polyaniline and its composites with LiFePO_4 and LiMn_2O_4 - Prospective cathode active materials for environment friendly and flexible Li-ion battery applications

Received 00th January 20xx,
Accepted 00th January 20xx

DOI: 10.1039/x0xx00000x

www.rsc.org/

Anand B. Puthirath^a, Bibin John^b, C. Gouri^b, S. Jayalekshmi^a

The present work is aimed at investigating the electrochemical properties of Li-ion cells, assembled using lithium substituted polyaniline and its composites with LiFePO_4 and LiMn_2O_4 as the cathode active materials. Lithium substitution in PANI can be achieved by a variety of approaches and the present work introduces one of the cost effective methods using a comparatively cheaper lithium salt, n-Butyllithium in hexane (n-BuLi) as the dopant. X-ray diffraction, FTIR and SEM techniques were used to get the structural and surface morphological details of the Li-substituted PANI (LIPO) samples. Coin cells were assembled in the glove box using LIPO as cathode and lithium metal foil as anode with 1 M LiPF_6 in EC: DMC (1:1) as electrolyte. Voltage sweep cyclic voltammetry and charge-discharge cycling were employed to characterize the electrochemical capabilities of the assembled cells. The cells are found to show a maximum discharge capacity of 25.04 mAh/g with 99.99 % columbic efficiency and have got tremendous cycling stability over 50 cycles. Pouch cells were assembled using LIPO samples as cathode active materials, graphite as anode and gel polymer (Poly (ethylene oxide)) as electrolyte. The pouch cells are found to hold the open circuit voltage of 0.6 V (OCV) even when bent up to 90° from the initial state, which provides the first signature of constructional flexibility of these polymer based Li ion cells. Hoping to improve the specific capacity of LIPO based cells, composite cathode materials were synthesized by mixing LIPO samples with LiFePO_4 and LiMn_2O_4 in 9:1 ratio by weight. The cells are found to show a maximum discharge capacity of 37 mAh/g with 99.99 % columbic efficiency and have got excellent cycling stability over 50 cycles. One of the highlights of these studies is the observation that the inherent Jahn Teller effect associated with LiMn_2O_4 cathode material can be eliminated to a great extent by making composites with LIPO samples.

Introduction

The development of conducting polymer based rechargeable Li-ion cells with high specific capacity and excellent cycling characteristics is a highly competitive area among research and development groups, worldwide. Polymer based rechargeable batteries are specifically attractive due to the environmentally benign nature and the possible constructional flexibility they offer. Conducting polymers generally have electronic band structure with π conjugated delocalized electrons spread along the polymer backbone. Conducting and semiconducting polymers have received immense attention since the discovery of high electrical conductivity in doped polyacetylene. In the category of conducting polymers, polyaniline (PANI), polypyrrole (PPY) and polythiophene (PTH) are examples of stable type electrically conducting polymers. Most of the research in the field of conducting polymers has concentrated on their applications in optoelectronic devices

like solar cells, light emitting diodes (LED), photoconductors, electrochromic displays and energy storage devices like battery and supercapacitors [1-9].

Polymers like PANI, PPY, and PTH are particularly expected to be active electrode materials for lithium secondary battery applications because they are stable in air and have good electrochemical properties. The use of conducting polymers as electrodes in Li-ion cells relies on their electrochemical redox (doping/dedoping) processes. A given polymer can be repeatedly cycled between different oxidation states, thereby acting as a reversible electrode for a rechargeable battery. Although in principle conducting polymers can be used both as anode (by exploiting their reduction or n-doping process) and cathode (by oxidation or p-doping), most battery applications are confined to the latter case. The electrochemical process, in most of the polymer based Li-ion cells, involves the Li-salt to an extent defined by the Li doping level or the extent of the oxidation state reached by the polymer electrode. The Li doping level is proportional to the amount of charge involved and directly related to battery capacity (Ah) [10].

^a Division for Research in Advanced Materials, Department of Physics, Cochin University of Science and Technology, Kochi, Kerala, India 68222.

^b Lithium Ion and Fuel Cell Division, Vikram Sarabhai Space Centre, Thiruvananthapuram-695022, Kerala, India

Another particular feature of conducting polymer based Li-ion cells is that the electrode kinetics is generally controlled by the diffusion of the dopant anions throughout the polymer structure. As expected, the charge-discharge rate of polymer electrodes greatly depends upon the nature (size and charge density) of the dopant anion and the electrode morphology. Therefore, the synthesis conditions of conducting polymers become very important for assuring their capability as electrodes in electrochemical cells. The polymer electrode configuration retains specific advantages such as flexibility in geometry and design, compatibility with the environment and the projected low cost which are factors that make them competitive for small sized, low rate button prototypes for the microelectronics consumer market [11-12]. The development of rechargeable battery systems having excellent charge storage capacity, cyclability, environmental friendliness and flexibility has yet to be realized in practice. Rechargeable Li-ion cells employing cathode active materials like LiCoO_2 , LiMn_2O_4 , LiFePO_4 have got remarkable charge storage capacity with least charge leakage when not in use. However, material toxicity, chance of cell explosion and lack of effective cell recycling mechanism pose significant risk factors which are to be addressed seriously. These cells also lack flexibility in their design due to the structural characteristics of the electrode materials [13, 14].

In the present work, attempts have been made to assemble rechargeable Li ion cells employing Li substituted (Li-doped) polyaniline as the cathode active material, lithium foil as anode and lithium hexafluorophosphate (LiPF_6) in ethylene carbonate (EC) : dimethyl carbonate (DMC) (1:1) as electrolyte. In earlier reports, using lithium substituted (lithiated) PANI as cathode, the lithiation has been achieved by treating PANI with LiPF_6 or LiBF_4 [2, 15-17]. In the present work lithiation has been effected by treating PANI with n-butyllithium (n-BuLi) in hexane which is a novel approach to achieve lithium substitution in PANI. The prime advantage of this technique is the much reduced material cost involved in the synthesis. The cost of n-BuLi is about 1/10 th of that of LiPF_6 and LiBF_4 . Structural and morphological studies on Li- substituted PANI, along with the electrochemical characterization have not been carried out extensively. Concentration of n-BuLi has been varied to get Li doped PANI samples with improved specific capacity. However it is observed that the charge storage capacity is not sufficient to meet the current industrial requirements.

Hence with a vision of increasing the charge storage capacity, we have synthesized LIPO- $\text{LiFePO}_4/\text{LiMn}_2\text{O}_4$ composites by mixing LIPO samples with $\text{LiFePO}_4/\text{LiMn}_2\text{O}_4$ in 9:1 ratio by weight using a mortar. The resultant products were used as the active material in cathode preparation. The cyclic voltammograms and charge-discharge characteristics of LIPO- $\text{LiFePO}_4/\text{LiMn}_2\text{O}_4$ composite cathode based coin cells were investigated and their capabilities compared.

Experimental

Synthesis

To start with, the emeraldine salt (ES) form of HCl doped PANI was synthesized via chemical oxidative polymerization method [18]. It was de-doped using NH_4OH solution to get the emeraldine base (EB) form of PANI. The resultant product was treated with "n-Butyllithium in hexane (n-BuLi)" in an argon filled glove box (99.999% purity) with moisture content less than 5 ppm, to get the lithiated form of PANI. The n-BuLi is expected to disaggregate the polyaniline clusters by binding the amines to its lithium centers and this process is referred to as metalation (figure.1). Concentration of the n-BuLi was varied in three steps to achieve improved metalation [19]. The reaction mechanism is illustrated in figure1. Resultant products are named as LIPO 1, LIPO 2 and LIPO 3 respectively. These samples were subjected to detailed structural characterization. Coin cells were assembled in the glove box using LIPO 1, LIPO 2 and LIPO 3 as cathode active materials, lithium metal foil as anode, porous polyethylene film as separator and 1 M LiPF_6 in EC: DMC (1:1) as electrolyte. The charge collector (Al foil), LIPO electrode, separator/electrolyte solution, lithium metal electrode, and charge collector (Al mesh) were assembled in sequence as a sandwich and enveloped in a laminated-stainless steel button type cap (2032) inside an argon filled glove box. The assembled coin cells were characterized to assess the electrochemical capabilities.

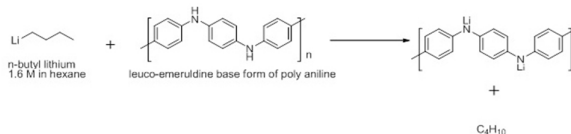


Figure.1: Possible mechanism of partial metalation process

LIPO 1, LIPO 2 and LIPO 3 were used to make composites with $\text{LiFePO}_4/\text{LiMn}_2\text{O}_4$ in 9:1 proportion by weight. They were named as LiFe 1, LiFe 2 and LiFe 3 and LiMO 1, LiMO2 and LiMO3 respectively. LIPO- $\text{LiFePO}_4/\text{LiMn}_2\text{O}_4$ composites with 10 % conductive additives and the PVDF binder were coated on battery grade aluminium foils and dried for 3 h at 60°C under dynamic vacuum. The electrochemical cells were assembled using LIPO- $\text{LiFePO}_4/\text{LiMn}_2\text{O}_4$ powder as the active material for the positive electrode as explained earlier.

Characterisations

Thermo Electron IRIS INTREPID II XSP DUO model ICP-AES system was used for the qualitative and quantitative determination of the presence of lithium in the samples. X-ray diffraction (XRD) employing Rigaku Dmax C diffractometer with Cu K α radiation of 1.54 Å was used for the structural characterization of the samples. A Thermo Nicolette Avatar 370 DTGS model Fourier Transform IR (FTIR) spectrophotometer was used to obtain the IR spectrum of the samples in the range 400–4000 cm^{-1} . JEOL Model JSM - 6390LV Scanning Electron Microscope (SEM) was used to generate surface morphological images of the samples with the resolution of a micrometre.

Cyclic Voltammetry experiment was carried out employing the Biologic SP300 research grade potentiostat / galvanostat. Charge-discharge test was carried out between 2V and 4 V using 8 channel battery analyser (5V, 1 mA-MTI Corporation USA) at C/10 current rate.

Results and discussions

Lithiated Polyaniline (LIPO)

Inductively Coupled Plasma Atomic Emission (ICP-AES) Analysis

In this instrument, the atomic spectrum emitted by a sample is used to determine its elemental composition. The wavelength at which emission occurs is used to identify the element, and the intensity of the emitted radiation quantifies its concentration [20]. LIPO 1, LIPO 2 and LIPO 3 samples were digested using 5ml HNO₃ and made up into 100ml using HPLC grade water and were analysed using ICP-AES system. Results of the analysis are tabulated in Table 1. It can be seen that on increasing the n-BuLi concentration, the lithium content in the sample is getting increased. However the metalation is partial and the maximum metalation achieved is 15.39%. The behaviour of Li enrichment with n-BuLi doping concentration is shown in figure.2.

Sample Name	Lithium Content (%)
LIPO 1	10.04
LIPO 2	13.61
LIPO 3	15.39

Table 1: ICP-AES Measurement Data

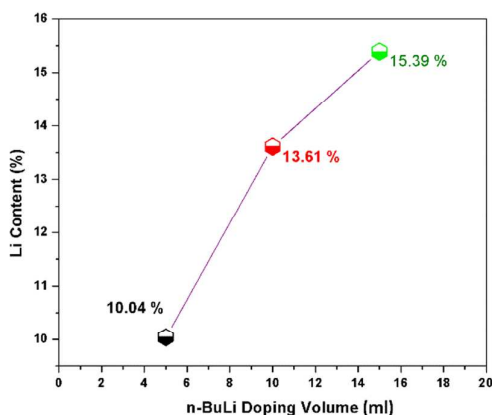


Figure 2. Variation of lithiation with respect to n-BuLi doping concentration

X-Ray Diffraction studies

On studying the powder diffraction data shown in figure 3, it is clear that emeraldine base form of PANI shows broad peaks around 2θ values of 11° , 17° and 21° [21] which agree with the already reported data. For lithiated samples, instead of broad peaks indicating amorphous structure, intense and narrow

peaks are seen around 11° and 21° with additional diffraction peaks at 30° , 33° , 37° , 50° . The presence of these peaks indicates a semi crystalline nature for all the lithiated samples. Better crystalline nature of these lithiated PANI samples compared to normal PANI is a good sign of better structural order, which in turn is helpful to sustain the structural integrity during Li ion exchange.

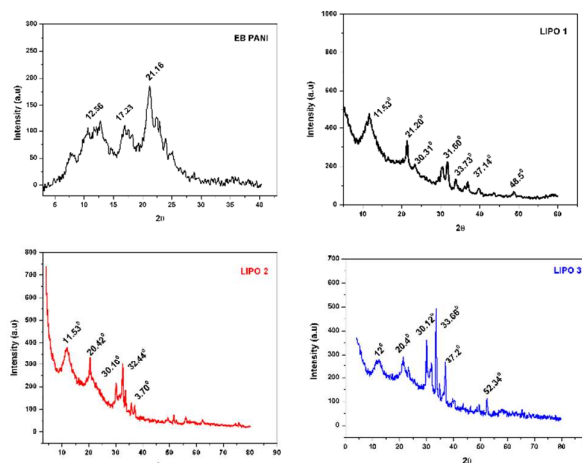


Figure 3: X- ray diffraction patterns of EB PANI and lithiated PANI samples

FTIR Analysis

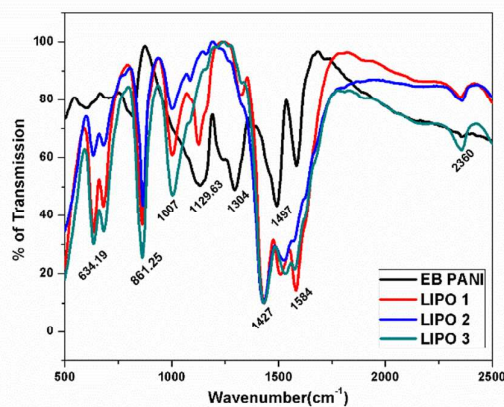


Figure 4: IR transmission curves of EB PANI and lithiated PANI samples

The IR response of the emeraldine base form of PANI and the lithiated samples is illustrated in figure 4. In PANI, the characteristic peaks at 1584cm^{-1} and 1497cm^{-1} correspond to the quinoid ring (Q) and the benzenoid ring stretching modes respectively. It can be seen that for lithiated samples, the peak at 1584cm^{-1} is broadened enough to be hardly considered as the signature of quinoid stretching. The characteristic peak of polyaniline base is the N=Q=N stretching band at 1129cm^{-1} [22]. The bands in the range $1200\text{--}1400\text{cm}^{-1}$ represent the C–N stretching modes of the aromatic ring. For the lithiated samples, vibration modes at 1304cm^{-1} and

1497 cm^{-1} are absent which are of secondary aromatic amine stretching and benzenoid ring stretching respectively. These modes are signatures of the presence of amine and imine groups in the sample. It is seen that on lithiation these modes become very feeble to be detected by the sensor. This is a strong evidence for lithium substitution of PANI although it is partial.

Microstructure Analysis-SEM

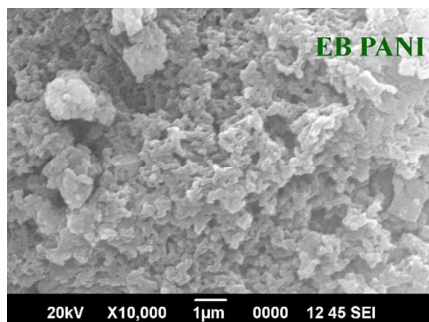


Figure 5: SEM image of EB PANI

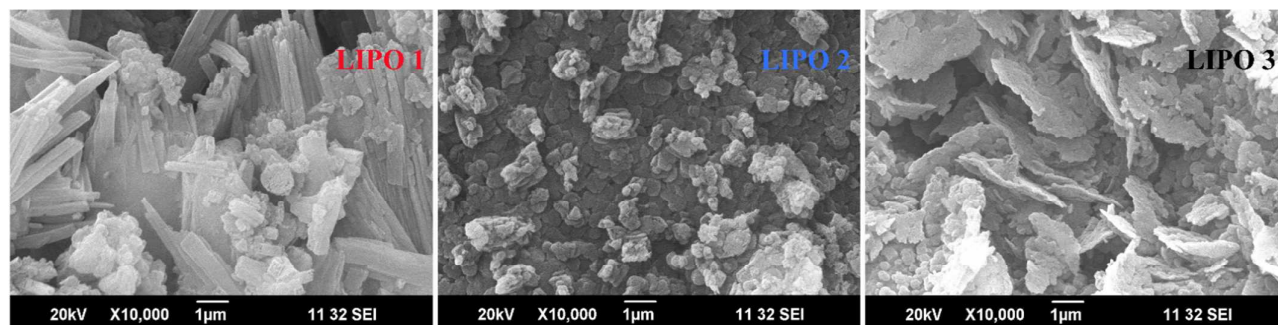


Figure 6: SEM images of LIPO 1, LIPO 2 and LIPO 3

The scanning electron microscope images of EB PANI and the three lithiated PANI samples are shown in figures 5 and 6 respectively. It is seen that surface morphology is considerably modified at the submicron level on increasing the n-BuLi concentration. For the lowest n-BuLi concentration, rod like structures are formed. For the medium n-BuLi concentration flake like structures are observed and for the highest n-BuLi concentration, the result is the formation of bigger flake like structures. Unlike the random distribution of polymer chains in EB PANI, on treating with n-BuLi, more ordered structures are formed in LIPO1, LIPO 2 and LIPO 3 samples, complementing the presence of crystalline peaks in the X-ray diffraction patterns of these samples. These ordered structures can comfortably sustain this morphology during Li ion exchange process with a healthy Li ion transport.

Electrical Conductivity Studies

The DC electrical conductivity of the samples was studied using two probe technique, employing Keithley source meter, interfaced to a computer using Lab-View program. The

current-voltage (I-V) curves for different concentrations of n-BuLi, with the calculated conductivity values, are shown in Figure 7. Conductivity of the samples shows only a marginal increase on treating with n-BuLi. However the conductivity values obtained are in the expected range for cathode active materials.

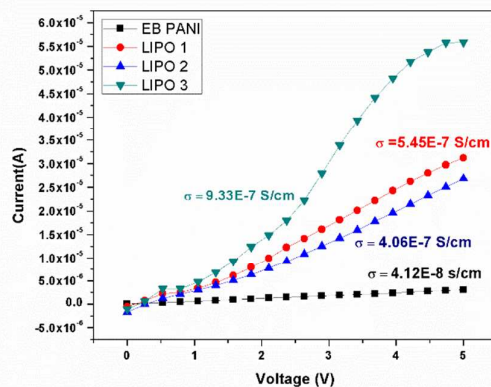


Figure 7: I-V curves of the samples for different n-BuLi concentration along with the calculated conductivity values

Cyclic Voltammetry Analysis

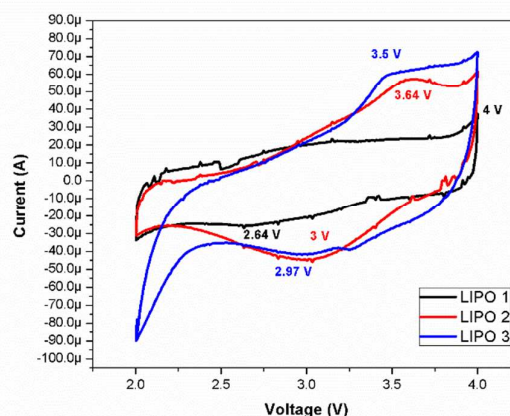


Figure 8: Voltage sweep cyclic voltammetry response of LIPO 1, LIPO 2 and LIPO 3

The cyclic voltammetry studies were carried out on coin cells assembled in the glove box using lithiated PANI as cathode and Li metal as anode. The cyclic voltammetry curves of the LIPO 1,

LIPO 2 and LIPO 3 samples are shown in figure 8. The response curves for voltage scan between 2V to 4V show reversible characteristics with broad peaks corresponding to cathodic and anodic scans. The cathodic peak corresponds to one step Li oxidation process to form Li deficient PANI with the release of an electron from the cathode. The anodic peak corresponds to the reduction of Li ion with the insertion of Li back into cathode. It is seen that, the oxidation potential is in the range 3.5V- 4 V and the reduction potential falls between 2.6 V to 3.5 V. The cathodic and anodic peaks become more prominent and resolved as the percentage of lithiation increases. The area of the CV curve also increases with increase in the percentage of lithiation. The open circuit voltage of the assembled coin cells is around 3.5 V.

Charge Discharge Cycle Analysis

The theoretical capacity of lithiated polyaniline is 142 mAh/g which corresponds to 100 % lithiation [23]. In the present work, maximum lithiation achieved is only 15 %. Hence the theoretical capacity expected is around 25 mAh/g. The maximum specific capacity of 25.04 mAh/g is obtained for LIPO 3 sample with the maximum Li substitution around 15 %. Lithiated PANI based Li-ion cells with fairly good specific capacity close to theoretical capacity, coulombic efficiency close to 100 % and excellent cycling stability have not been reported earlier. In the present case, LIPO 3 sample shows the maximum capacity of 25.04 mAh/g for the first cycle and then shows a decreasing nature for a few following cycles. After the fifth cycle onwards, the capacity remains the same up to the 50th cycle. In the case of the other two samples, for the first few cycles, a capacity in the range 13 mAh/g – 16.5 mAh/g is observed and thereafter there is a fall in capacity till the 10th cycle. Then the capacity shows no fading for the rest of the cycles until the 50th. The charge-discharge curves of the three cells are shown in figure 9 and the specific capacities are plotted in figure 10.

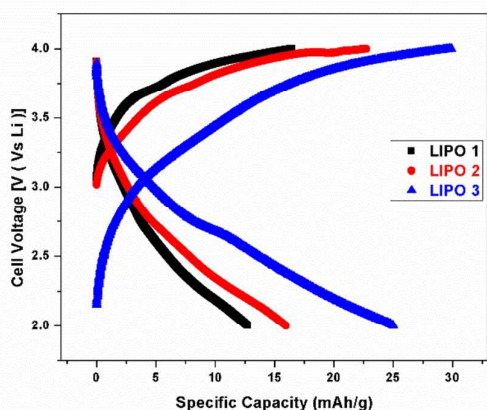


Figure 9: Charge-discharge curves of LIPO 1, LIPO 2 and LIPO 3

After the 5th and 10th charge discharge cycles, all the three samples show a stable cycling behaviour. All the three samples

show coulombic efficiency close to 99 % for all the charge discharge cycles.

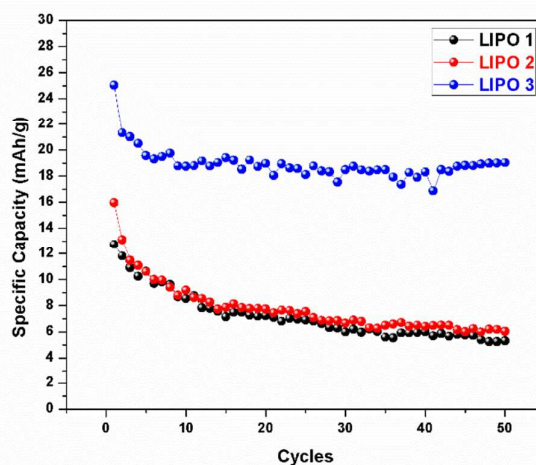


Figure 10: Specific capacity versus charge-discharge cycle number for LIPO 1, LIPO 2 and LIPO 3

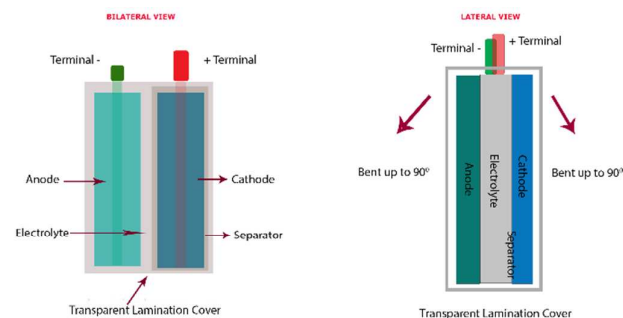


Figure 11: Schematic representation of pouch cells assembled with LIPO 1, LIPO 2 and LIPO 3

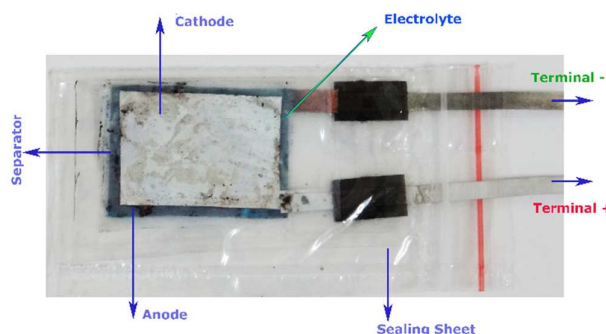


Figure 12: Pouch cell assembled with LIPO 1, LIPO 2 and LIPO 3

Pouch cells were assembled using LIPO samples as cathode, graphite as anode [24] and gel polymer (Poly(ethylene oxide)) as electrolyte [25,26]. Schematic diagrams of the assembled cells are shown in figure.11 and the realised pouch cell is shown in figure. 12. The pouch cells are found to hold the open circuit voltage of 0.6 V (OCV) even when they are bent up to 90^o from the initial state. This gives the first signature of flexibility associated with polymer based Li-ion cells.

Lithiated-Polyaniline-LiFePO₄ Composite (LiFe)

X-ray Diffraction Study

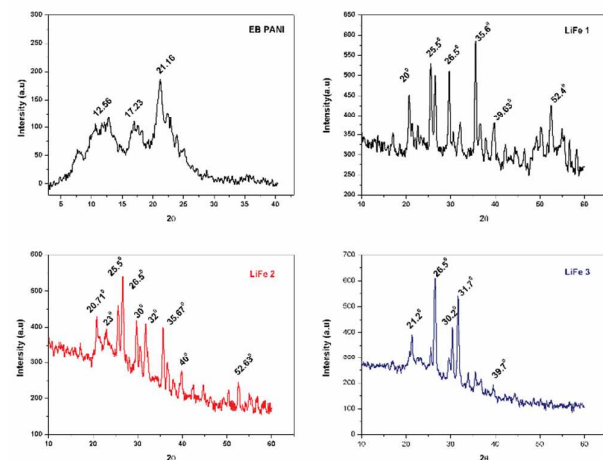


Figure 13. The XRD spectrum of EB PANI, LiFe1, LiFe 2 and LiFe 3

X-ray diffraction patterns of LIPO- LiFePO₄ composite samples are shown in figure 13. The patterns consist of the characteristic peaks of both Lithiated PANI and LiFePO₄. Characteristic peaks of LIPO are well evident from the XRD patterns. There are also peaks corresponding to 20⁰ (101), 25⁰ (201, 111), 30⁰ (211, 020), 35⁰ (311) which give the clear evidence for the presence of LiFePO₄ in the composite system [27].

Cyclic Voltammetry studies

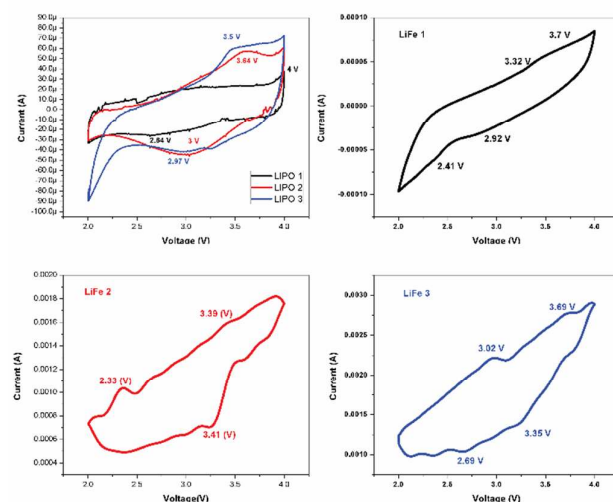


Figure 14: Cyclic voltammograms of LIPO, LiFe 1, LiFe 2 and LiFe 3

In order to identify oxidation/reduction potentials and study the electrochemical capability of the cells assembled using LiFe composite cathodes, cyclic voltammetry was performed. The oxidation and reduction peaks of these systems occur within 2 to 4 V and show good reversibility. For these LiFe cells, the upper two broad peaks (~3.32 and ~3.7 V) correspond to the oxidation and the lower two broad peaks (~2.82, and ~2.41 V)

to the reduction as shown in figure 14. There are two broad peaks in oxidation stage and two broad peaks in reduction stage for LiFe systems. The upper peak at ~3.32 V corresponds to the oxidation of Li in lithiated PANI and that at 3.7 V to the oxidation (de-intercalation of Li⁺ ion) of Li in LiFePO₄ and the lower peaks at ~2.82 and ~2.18 V correspond to the reduction of LIPO and that (intercalation of Li⁺ ion) of LiFePO₄ respectively [12].

Charge Discharge Analysis

The discharge characteristics of LiFe 1, LiFe 2 and LiFe 3 cells are shown in figure 15. These discharge curves resemble those of transition metal oxide electrodes in conventional rechargeable lithium ion cells. The average operating voltage of these cells may be approximated to 3.3 V in spite of different LIPOs used. Figure 16 shows the discharge capacity Vs number of cycle curves of LiFe (1-3) samples. The highest discharge capacity is around 40 mAh/g for LiFe 3 followed by 25 mAh/g for LiFe 2 and 21 mAh/g for LiFe 1.

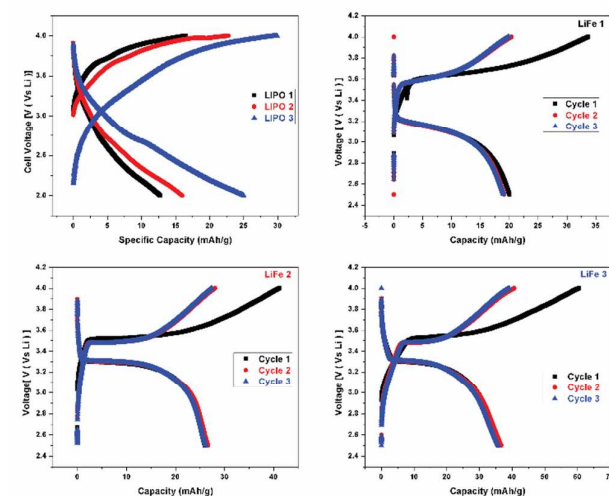


Figure 15: Charge-discharge curves of LIPO, LiFe 1, LiFe 2 and LiFe 3 cells.

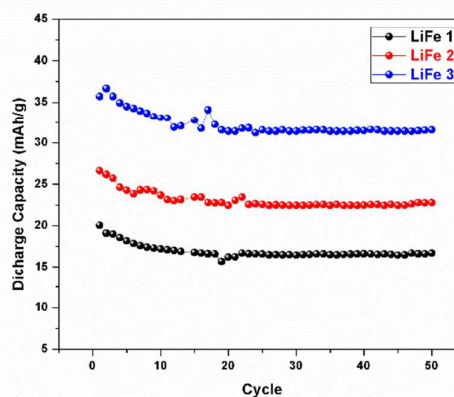


Figure 16: Discharge Capacity Vs Number of cycle curves of LiFe 1, LiFe 2 and LiFe 3 cells

Figure 17 shows the charge efficiency of the assembled coin cells. All the cells show an average efficiency around 98%. The observed values are very impressive and can be compared with those of the conventional Li-ion secondary battery systems.

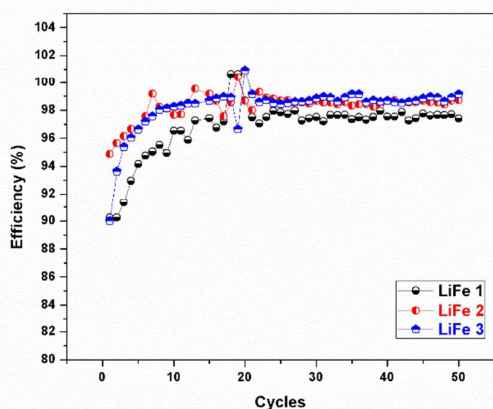


Figure. 17: Charge Efficiency Vs. Number of cycle curves of LiFe 1, LiFe 2 and LiFe 3 cells

Lithiated-Polyaniline- LiMn_2O_4 Composite (LiMO)

X-Ray Diffraction Study

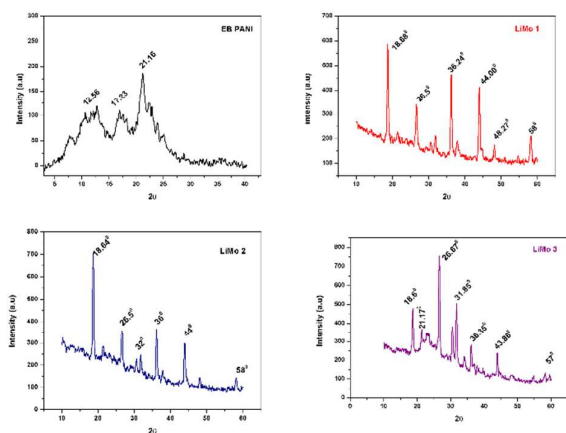


Figure.18: X-ray diffraction patterns of EB PANI, LiMO 1, LiMO 2 and LiMO 3

X-ray diffraction patterns of LIPO- LiMn_2O_4 composite samples are depicted in figure.18 and they consist of the characteristic peaks of both Lithiated PANI and LiMn_2O_4 . Major peaks of LiMn_2O_4 at 20° (111), 36° (311), 45° (400), 59° (511) are present in the XRD patterns. Generally on cycling, LiMn_2O_4 which has spinel structure, slowly gets transformed to the tetragonal phase compound, leading to poor cyclability of the electrode. This drawback, its inability to sustain the charge capacity over the charge discharge cycles, due to Jahn–Teller effect may be overcome by mixing LiMn_2O_4 with suitable Li-containing conducting polymer based materials [28].

Cyclic voltammetry

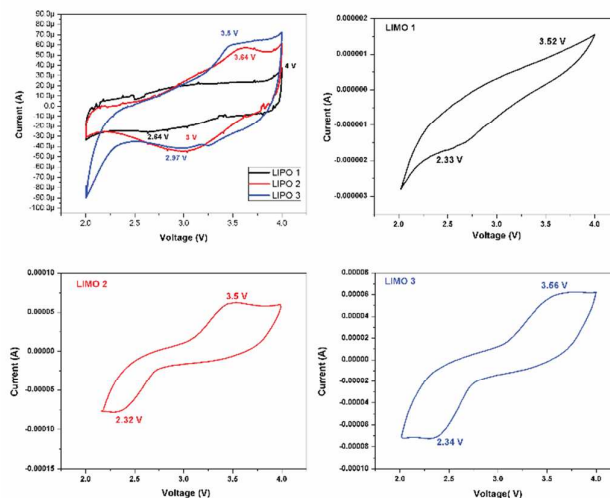


Figure. 19: Cyclic voltammograms of LiPO, LiMO 1, LiMO 2 and LiMO 3

The oxidation and reduction peaks of these cells occur within 2 to 4 V and show good reversibility. The upper broad peak at ~ 3.5 V is common to both LIPO and LiMn_2O_4 which corresponds to the oxidation of Li in lithiated PANI and that (de-intercalation of Li^+ ion) in LiMn_2O_4 . The lower broad peak at ~ 2.32 V is also common to both LIPO and LiMn_2O_4 which corresponds to the reduction in these components of the composite systems.

Charge Discharge Characteristics

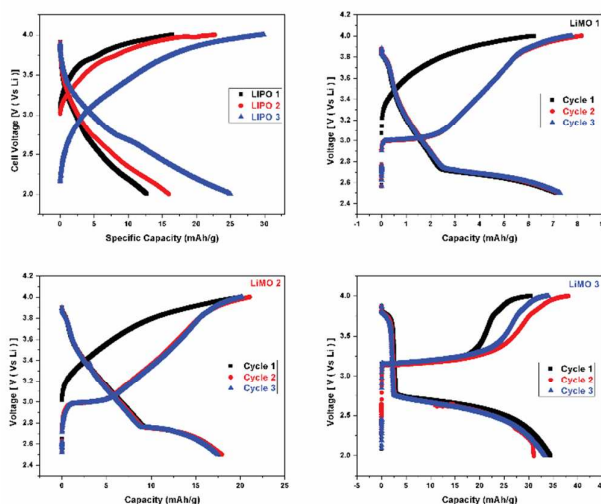


Figure. 20: Charge-discharge curves of LiMO 1, LiMO 2 and LiMO 3 cells

The discharge characteristics of LiMO 1, LiMO 2 and LiMO 3 based cells are shown in figure 20. These discharge curves also resemble those of transition metal oxide electrodes in

conventional rechargeable lithium ion cells. The operating voltages of these cells can be approximated to 3.0 V in spite of different LIPOs used. Figure 21 shows the discharge capacity Vs cycle life curves of LiMO(1-3) cells. The highest discharge capacity is around 37 mAh/g for LiMO 3 based cell, followed by 20 mAh/g for LiMO 2 and 10 mAh/g for LiMO 1 based cells respectively. For all the cells assembled, the cycling stability over the first fifty cycles is quite remarkable and there is hardly any capacity loss. This could be the result of the nullifying of the Jahn–Teller distortion in LiMn_2O_4 due to the presence of lithiated PANI in the cathode material.

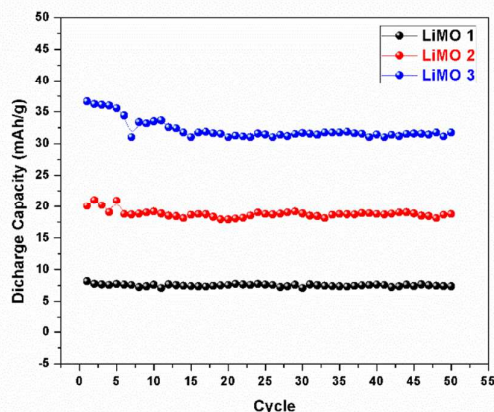


Figure. 21: Discharge Capacity Vs Cycle number curves of LiMO 1, LiMO 2 and LiMO 3 cells

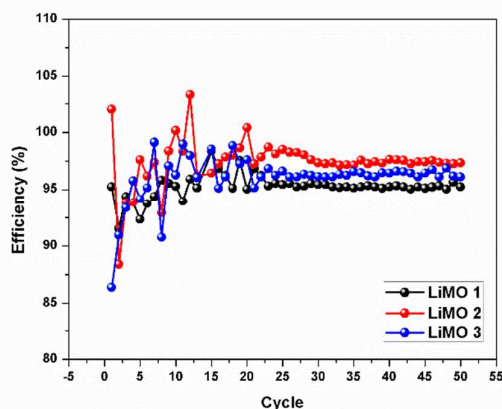


Figure. 22: Charge Efficiency Vs Cycle number curves of LiMO 1, LiMO 2 and LiMO 3 cells

Figure 22 shows the charge efficiency of assembled coin cells. It is seen that the efficiency of the cells show an increasing tendency till the 10th cycle. There after the efficiency of the cells stabilizes to a fixed value around 98%.

Conclusions

The present work highlights the suitability of using n-butyllithium, a cost effective substitute for expensive counterparts like LiPF_6 and LiBF_4 , for synthesizing Li substituted

polyaniline to be used as the cathode active material in rechargeable Li ion cells. The structural analysis confirms the enhanced crystallinity/order in Li substituted samples compared to pure PANI. The coin cells assembled using Li substituted PANI as cathode show quite good electrochemical behaviour. Specific capacity close to the expected theoretical capacity has been obtained for all the cells fabricated. All the three assembled cells show excellent columbic efficiency around 99% and stable charge discharge cycling behaviour up to 50 cycles. The pouch cells assembled using lithiated PANI as cathode are found to hold the open circuit voltage (OCV) even when bent up to 90° from the initial state. This will open up a new methodology to fabricate all solid state, flexible and environmentally friendly lithium ion cells. However, the capacity of the lithiated PANI based cells have to be improved still further to meet the current industrial standards. For that, Lithiated PANI (LIPO 1, LIPO 2 and LIPO 3)- LiFePO_4 / LiMn_2O_4 (9:1 ratio) composite electrodes based Li-ion cells were assembled and detailed electrochemical characterization was carried out. The cells assembled with LIPO 3- LiFePO_4 / LiMn_2O_4 composites as active electrodes show dominant electrochemical characteristics over LIPO1- LiFePO_4 / LiMn_2O_4 and LIPO 2- LiFePO_4 / LiMn_2O_4 based cells. The average voltage of these cells is around 3.3 V. The cells are having the highest discharge capacity around 40 mAh/g and columbic efficiency around 97% and have got tremendous capacity retention over 50 cycles. Unlike pure LiMn_2O_4 based cells with poor cyclability due to Jahn–Teller distortion, LiMO cells have been found to overcome this distortion effect and show healthy cycling stability, due to the presence of lithiated PANI in the cathode material. The present work highlights a novel but simple approach to nullify the Jahn Teller distortion in LiMn_2O_4 by properly mixing it with Lithiated PANI to function as the cathode. On optimizing the n-BuLi doping concentration and LIPO- LiFePO_4 / LiMn_2O_4 mixing ratios, polymer based Li-ion hybrid cells having promising energy density, capacity and eco friendliness with structural flexibility can be realized.

Acknowledgment

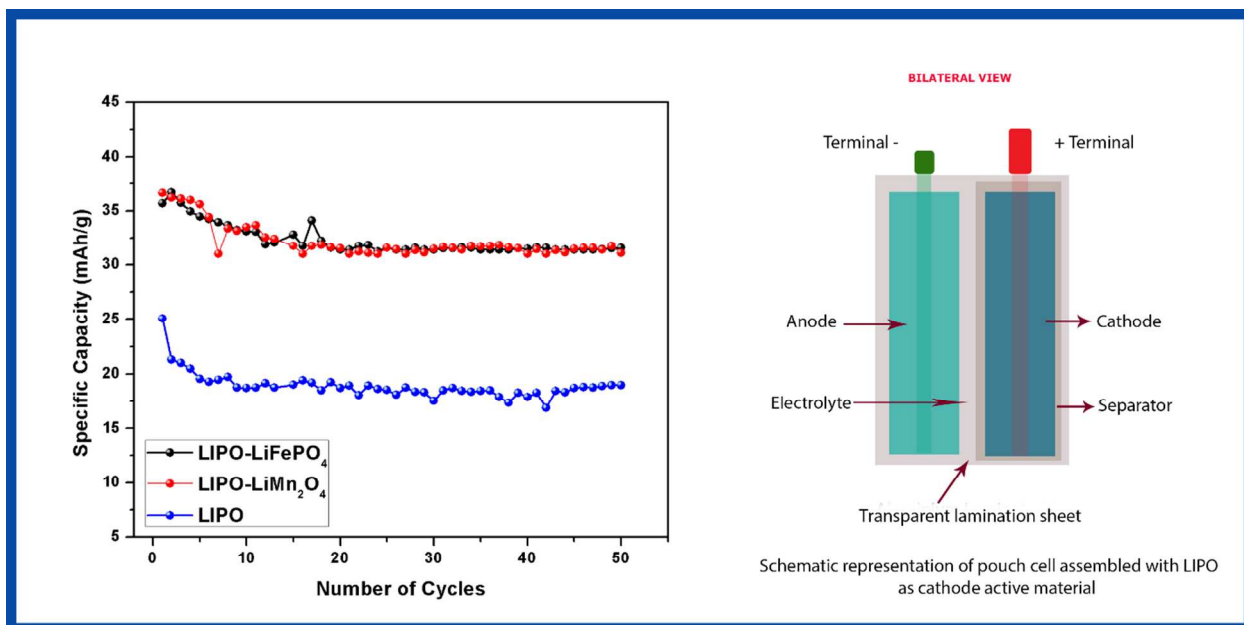
The financial assistance provided by the Board of Research in Nuclear Sciences (BRNS), Government of India, is gratefully acknowledged.

References

- Ito, T.; Shirakawa, H.; Ikeda, S. *J. Polym. Sci. Polym. Chem.* 1974, **12**, 11.
- Nigrey, P. J.; MacInnes, D. Jr.; Nairns, D. P.; MacDiarmid, A. J. *J. Electrochem. Soc.* 1981, **128**(8), 1651.
- Panero, S.; Prosperi, P.; Bonino, F.; Scrosati, B.; Corradini, A.; Mastragostino, M. *Electrochim. Acta* 1987, **32**(7), 1007.
- Nishio K.; Fujimoto M.; Yoshinaga N.; Furukawa N.; Ando O.; Ono H.; Suzuki, T. *J. Power Sources.* 1991, **34**, 153.
- Loufty, R. D.; Sharp, J. H. *J. Chem. Phys.* 1979, **71**(3), 1211.
- Jelle, B. P.; Hagen, G.; Nodland, S. *Electrochim. Acta.* 1993, **38**(11), 1497.
- Bao, Z.; Feng, Y.; Dodabalpu, A.; Raju, V. R.; Lovinger, A. *J. Chem. Mater.* 1997, **9**(6), 1299.

8. Muhammad E. Abdelhamid, Anthony P. O'Mullane and Graeme A. Snook, *RSC Adv.*, 2015, **5**, 11611-11626
9. Prakash Sengodu and Abhay D. Deshmukh, *RSC Adv.*, 2015, **5**, 42109-42130
10. Arbizzani, C.; Mastragostino, M.; Scrosati, B. Handbook of Organic Conductive Molecules and Polymers; Nalwa, H. S., Ed.; John Wiley & Sons Ltd.: 1997; Ch. 11.
11. Osaka, T.; Naoi, K.; Ogano, S. *J. Electrochem. Soc.* 1988, **135**, 5, 1071
12. Kwang Sun Ryu et al, *Bull. Korean Chem. Soc.* 2002, **23**, 8
13. Masaki Yoshio, Ralph J. Brodd, Akiya Kozawa, Lithium-Ion Batteries, Science and Technologies, *Springer XXVI.*, 2009; 452:279.
14. Bo Xu, Danna Qian, Ziyang Wang, Ying Shirley Meng, *Materials Science and Engineering.*, 20012, **73**, 51-65.
15. Panero, S.; Prospero, P.; Bonino, F.; Scrosati, B.; Corradini, A.; Mastragostino, M. *Electrochim. Acta.*, 1987; **32**(7), 1007.
16. Nishio, K.; Fujimoto, M.; Yoshinaga, N.; Furukawa, N.; Ando, O.; Ono, H.; Suzuki, T. *J. Power Sources*, 1991, **34**, 153.
17. Kwang Sun Ryu et al. *Synthetic Met.*, 2000; **110**, 213-217
18. Irina Sapurina and Jaroslav Stejskal, Review, *Polym Int.*, 2008; **57**, 1295-1325
19. Miah, M. A.; Snieckus, V. *J. Org. Chem.*, 1985; **50**, 5436.
20. Thomas J. Manning and William R. Grow, The chemical educator, *Springer-Verlag S.*, 1997; 1430-4171.
21. A. Mani, K. Athinarayanasamy, P. Kamaraj, S. Tamil Selvan, S. Ravichandran, K. L. N. Phani, S. Pitchumani, *J Mater Sci Lett.*, 1995; **14**(22), 1594-1596
22. Miroslava Trchova and Jaroslav Stejskal, *Pure Appl. Chem.*, 2011; **83**, 1803-1817.
23. K.S. Ryu, K.M. Kim, *J. Power Sources.*, 2007; **165**, 420-426
24. C. P. Sandhya, Bibin John, C. Gouri, *Ionics* 2014 **20**, 601-620
25. J.Y. Song, Y.Y. Wang, C.C. Wan, *J. of Power Sources* 1999, **77**, 183-197
26. Anand B. Puthirath, Bibin John, C. Gouri, S. Jayalekshmi, *Ionics*, doi:2015, 10.1007/s11581-015-1406-2
27. Lin Lin, Yaqiong Wen, Junke O, Yong Guo and Dan Xiao, *RSC Adv.*, 2013, **3**, 14652-14660
28. Rajive M. Tomy n, K.M. Anil Kumar, P.B. Anand, S. Jayalekshmi, *J. Phys. Chem. Solids*, 2011, **72**, 1251-1255

Table of Contents



The present work is an attempt to realize Li-ion cells using Li-substituted polyaniline (PANI) and its composites with LiFePO₄ and LiMn₂O₄ as cathodes, with flexibility in the cell design and the retention of capacity over long cycles.